

## A NEW PUNCHING SHEAR REINFORCEMENT SYSTEM FOR PRECAST FOOTINGS

**Dominik Kueres, M.Sc.**, Institute of Structural Concrete, RWTH Aachen, Germany

**Dr.-Ing. Marcus Ricker, M.Sc.**, HALFEN GmbH, Germany

**Univ.-Prof. Dr.-Ing. Josef Hegger**, Institute of Structural Concrete, RWTH Aachen, Germany

### ABSTRACT

*The punching shear resistance of reinforced concrete footings without shear reinforcement mainly depends on flexural reinforcement ratio, concrete compressive strength, and footing's dimensions (e.g. effective depth, shear span-depth ratio, size effects). Especially the increase of the effective depth enhances the punching shear resistance significantly and leads for in-situ casted footings to an economic design. For precast footings, the possible dimensions are limited due to transport reasons. Hence, a punching shear failure normally can only be prevented by installation of punching shear reinforcement.*

*Due to crack formation and fracture kinematics of compact footings, punching shear reinforcement systems with inclined bars seems to be more efficient than usual vertical bars. The present paper summarizes the results of seven punching tests conducted on footings with a new punching shear reinforcement system and practical dimensions. The high load-increase of 147% compared to identical footings without punching shear reinforcement is approximately 40% higher than for stirrups which underlines the potential of this new reinforcement system.*

**Keywords:** reinforced concrete, footings, punching shear, shear span-depth ratio, specific column perimeter, inclined punching shear reinforcement

## INTRODUCTION

Experimental investigations<sup>1-8</sup> on the punching shear behavior of reinforced concrete footings without shear reinforcement showed that the punching shear resistance mainly depends on flexural reinforcement ratio, concrete compressive strength, and footing's dimensions (e.g. effective depth, shear span-depth ratio, size effects). Especially the increase of the effective depth enhances the punching shear resistance significantly and leads for in-situ casted footings to an economic design. For precast footings, the dimensions are limited due to transport reasons. Hence, a punching shear failure normally can only be prevented by installation of punching shear reinforcement.

While vertical punching shear reinforcement elements like stirrups<sup>9-11</sup> and double-headed studs<sup>12-15</sup> significantly increase the punching shear resistance of flat slabs, this load-increase is less pronounced for footings<sup>7-8</sup>. Due to crack formation and fracture kinematics, a higher effectiveness of inclined punching shear reinforcement elements can be assumed. A punching test on a reinforced concrete footing with bent-down bars seems to confirm this assumption<sup>4</sup>.

Based on the results of previous test series<sup>4,6-8</sup>, a new punching shear reinforcement system with inclined bars was developed. In the present study, the effectiveness of the new punching shear reinforcement system is verified. A series of seven punching tests on reinforced concrete footings was conducted. All test specimens were provided with the new punching shear reinforcement system. The main parameters investigated in this test series were the layout of the punching shear reinforcement, the shear span-depth ratio  $a/d$ , the specific column perimeter  $u_0/d$ , and the effect of longitudinal reinforcement at the compression side.

## EXPERIMENTAL INVESTIGATIONS

The experimental program included seven tests on reinforced concrete footings. The tests were planned considering the results of a systematic test series on reinforced concrete footings without and with stirrups as punching shear reinforcement<sup>6-8</sup>. In all test specimens, a new punching shear reinforcement system with inclined bars and diameters of either 10 mm (0.4 in.) or 12 mm (0.5 in.) was installed. The notations DF\_N1 to DF\_N7 were used for the test specimens.

## MATERIALS

For all test specimens, commercial ready mixed concrete was used. The maximum coarse aggregate size was 16 mm (0.6 in.). Ordinary CEM II 42.5 R Portland cement and a water-cement-ratio ( $w/c$ ) of 0.68 to 0.72 were used, resulting in a slump between 470 mm (18.5 in.) and 520 mm (20.5 in.). The concrete mixture was designed to produce a 28-day target cylinder strength of  $f_{c,cyl} = 24$  MPa (3481 psi). To prevent premature failure, ultra-high performance concrete (UHPC) with concrete compressive strengths between  $f_{c,cyl} = 110.0$  MPa (15954 psi) and 129.6 MPa (18797 psi) was used for the column stubs. Additionally, the column stubs were reinforced with a steel collar made of 10 mm (0.4 in.) steel plates.

For all test specimens, the flexural reinforcement consisted of high grade steel St 900/1100 with yield strengths varying from  $f_y = 1034$  MPa (150.0 ksi) to 1044 MPa (151.4 ksi), a tensile strength of approximately  $f_t = 1217$  MPa (176.5 ksi), and a Young's modulus of approximately  $E_s = 194600$  MPa (28224 ksi). The high grade steel was used to prevent a premature flexural failure. The new punching shear reinforcement system was produced of steel B 500B, with measured yield strengths varying from  $f_y = 547$  MPa (79.3 ksi) to 585 MPa (84.9 ksi), tensile strengths in a range of  $f_t = 611$  MPa (88.6 ksi) and 653 MPa (94.7 ksi), and a Young's modulus between  $E_s = 194900$  MPa (28268 ksi) and 199800 MPa (28979 ksi). Table 1 summarizes the properties of the materials used.

Table 1 Details of test specimens and failure loads

Test	$h$	$d$	$c$	$b$	$u_0/d$	$a/d$	$f_{c,cyl}$	$\emptyset$	$f_y$	$\rho_l$	Top rft	$\emptyset_v$	$f_{yt}$	Layout	$V_{Flex}$	$V_{Test}$
	m (in.)	m (in.)	m (in.)	m (in.)	-	-	MPa (psi)	mm (in.)	MPa (ksi)	%	-	mm (in.)	MPa (ksi)	-	kN (kips)	kN (kips)
DF_N1	0.45 (17.7)	0.40 (15.7)	0.20 (7.9)	1.80 (70.9)	2.00	2.00	22.5 (3263)	20 (0.8)	1044 (151.4)	0.79	Yes	12 (0.5)	585 (84.9)	I	9862 (2217)	4082 (918)
DF_N2	0.45 (17.7)	0.40 (15.7)	0.20 (7.9)	1.80 (70.9)	2.00	2.00	22.6 (3277)	20 (0.8)	1044 (151.4)	0.79	No	12 (0.5)	585 (84.9)	I	9872 (2219)	4054 (911)
DF_N3	0.45 (17.7)	0.40 (15.7)	0.20 (7.9)	1.80 (70.9)	2.00	2.00	20.5 (2973)	20 (0.8)	1034 (150.0)	0.79	Yes	10 (0.4)	547 (79.3)	I	9566 (2151)	4544 (1022)
DF_N4	0.45 (17.7)	0.40 (15.7)	0.30 (11.8)	1.90 (74.8)	3.00	2.00	20.4 (2959)	20 (0.8)	1034 (150.0)	0.83	Yes	10 (0.4)	547 (79.3)	I	11297 (2540)	5045 (1134)
DF_N5	0.45 (17.7)	0.40 (15.7)	0.30 (11.8)	1.90 (74.8)	3.00	2.00	25.2 (3655)	20 (0.8)	1034 (150.0)	0.83	Yes	10 (0.4)	552 (80.1)	II	11905 (2676)	5937 (1335)
DF_N6	0.45 (17.7)	0.40 (15.7)	0.40 (15.7)	2.00 (78.7)	4.00	2.00	21.2 (3075)	20 (0.8)	1037 (150.4)	0.86	Yes	10 (0.4)	552 (80.1)	I	13285 (2987)	6515 (1465)
DF_N7	0.45 (17.7)	0.40 (15.7)	0.30 (11.8)	1.30 (51.2)	3.00	1.25	22.8 (3307)	20 (0.8)	1037 (150.4)	0.85	Yes	10 (0.4)	552 (80.1)	I*	14557 (3273)	6573 (1478)

$h$ : slab thickness;  $d$ : effective depth;  $c$ : square column dimension;  $b$ : square footing dimension;  $u_0/d$ : specific column perimeter;  $a/d$ : shear span-depth ratio;  $f_{c,cyl}$ : mean concrete compressive strength;  $\emptyset$ : diameter of longitudinal reinforcement;  $f_y$ : yield strength of longitudinal reinforcement;  $\rho_l$ : longitudinal reinforcement ratio; Top rft: Top reinforcement;  $\emptyset_v$ : diameter of shear reinforcement;  $f_{yt}$ : yield strength of shear reinforcement; Layout: Layout of punching shear reinforcement according to Fig. 1; I\*: only first row of punching shear reinforcement;  $V_{Flex}$ : shear force that produces flexural failure according to yield-line theory;  $V_{Test}$ : ultimate failure load.

## TEST SPECIMENS

The test series consisted of seven reinforced concrete footings with side dimensions of 1300, 1800, 1900, and 2000 mm (51.2, 70.9, 74.8, and 78.7 in.) in both directions and a thickness of 450 mm (17.7 in.). The square column stubs had side dimensions of 200, 300, and 400 mm (7.9, 11.8, and 15.7 in.) and were casted monolithically at the center of the footing. The effective depth was  $d = 400$  mm (15.7 in.) resulting in shear span-depth ratios between  $a/d = 1.25$  and 2.00, and specific column perimeters ranging from  $u_0/d = 2.00$  to 4.00. The flexural reinforcement ratio varied between  $\rho_l = 0.79\%$  and 0.86% and the diameter of the

inclined bars of the new punching shear reinforcement system was either 10 mm (0.4 in.) or 12 mm (0.5 in.). The different layouts of punching shear reinforcement investigated in this test series are shown in Fig. 1 for test specimens DF\_N4 (Layout I) and DF\_N5 (Layout II). Layout I consisted of eight punching shear reinforcement elements in the first row and eight punching shear reinforcement elements in the second row. In one test specimen (DF\_N5) only four punching shear reinforcement elements in the second row were installed.

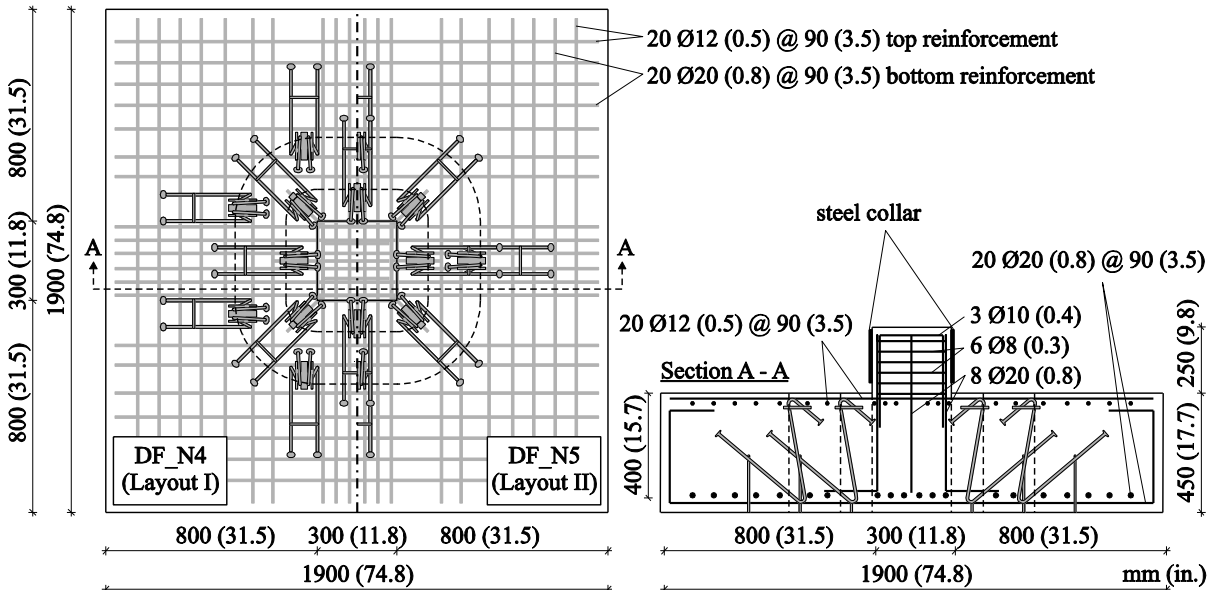


Fig. 1 Layout of flexural reinforcement and punching shear reinforcement for test specimens DF\_N4 and DF\_N5

## TEST SETUP AND MEASUREMENTS

The test specimens were loaded by a uniform surface load using the test setup shown in Fig. 2. The footings were tested upside down. A uniform pressure was simulated with 25 load application points. Twelve hydraulic jacks transferred their load through cross beams to two load points each. A further hydraulic jack with a piston area of half the size completed the load arrangement above the column. An equal distribution of the point loads was ensured since all hydraulic jacks were linked to the same oil circuit and applied the same load independently of the displacement. In order to avoid any formation of membrane forces in the test specimens, sliding and deformation bearings were placed between the footing and the cross beams.

During testing, the vertical displacement of the test specimens was recorded at the corners of the column stub and the footing's corners using linear variable differential transformers (LVDTs). To investigate the development of the inner shear cracks, the increase of the slab thickness was measured at several points and the penetration of the column into the slab was monitored. Strain gages were used to measure the strains in the flexural reinforcement and in the punching shear reinforcement. To obtain the average strain at the bar's axis, two strain gages were attached to opposite side faces of the reinforcing bars at each measuring point. The concrete strains were measured on the compression face of the footing near the column.

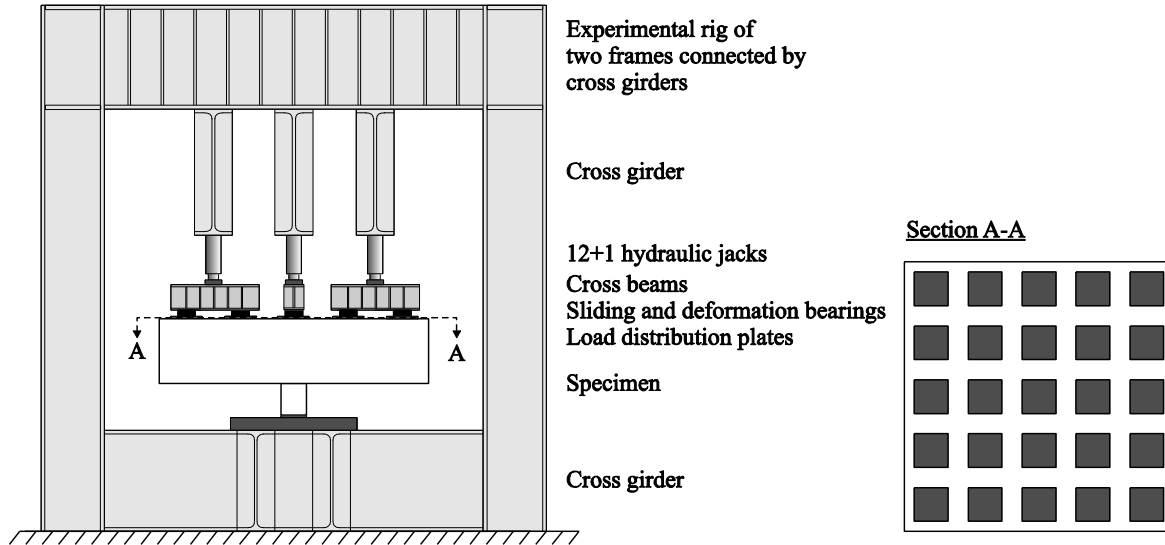


Fig. 2 Test setup

## TEST PROCEDURE

The load was applied force controlled in increments of 200 kN (44.9 kips). To simulate lifetime loading, the load was cycled ten times between a calculated service load and half its value. For the specimens DF\_N1, DF\_N2, and DF\_N3, the service load was 1200 kN (269.7 kips) corresponding to 40% of the maximum predicted failure load of an identical footing with stirrups according to DIN EN 1992-1-1+NA<sup>16,17</sup>. For the other test specimens, the service load was increased to 1400 kN (314.7 kips). After the load cycles, the test specimens were continuously loaded in a force controlled manner until final failure took place.

## EXPERIMENTAL RESULTS

All tests failed in punching of the footing, either as primary or secondary failure mechanism. The failure loads  $V_{Test}$  are listed in Table 1. The failure was initiated through an increasing slab thickness, increasing strains in the punching shear reinforcement, and a penetration of the column stub into the slab. The comparison with the flexural capacities of the footings  $V_{Flex}$  according to yield-line theory<sup>18</sup> (Table 1) reveals the fact, that the flexural capacities were not reached and hence confirms that failure occurred due to punching. Strain measurements verify this observation.

## CRACKING AND FAILURE CHARACTERISTICS

After testing, the footings were sawn into two halves to examine the inner crack patterns (Fig. 4). All crack patterns showed finely distributed shear cracks with inclinations between 22° and 78°. Regardless of the specific column perimeter  $u_0/d$ , the shear cracks propagated towards the column face. The saw-cuts of test specimens DF\_N1 (Fig. 3 (a)) and DF\_N2 (Fig. 3 (b)) with punching shear reinforcement consisting of 12 mm (0.5 in.) bars showed less

shear cracks than the other specimens with 10 mm (0.4 in.) bars (Fig. 3 (c-g)). The comparison of the crack patterns for specimens DF\_N4 (Layout I) (Fig. 3 (d)) and DF\_N5 (Layout II) (Fig. 3 (e)) showed more flat inclined shear cracks for specimen DF\_N5, especially outside the first row of punching shear reinforcement. Except for the short inclined bars in the second row, all bars of the punching shear reinforcement were crossed by many shear cracks and hence activated. Strain measurements confirm this observation. As observed in previous test series conducted on footings with stirrups as punching shear reinforcement<sup>6-8</sup>, the inclination of the shear cracks seems not to be affected by the shear span-depth ratio  $a_v/d$  (Fig. 3 (g)).

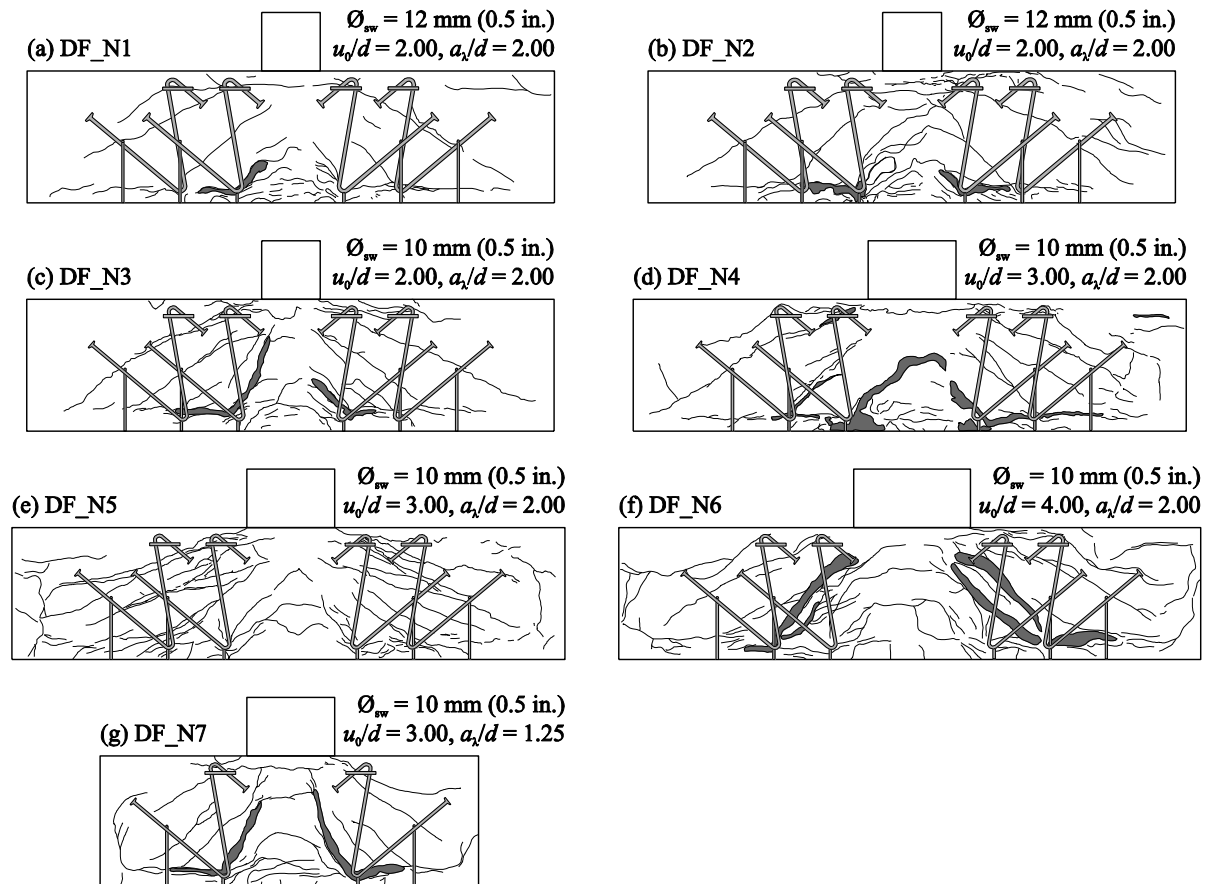


Fig. 3 Saw-cuts of the test specimens

## LOAD-DEFLECTION CHARACTERISTICS

In Fig. 4 (a), the comparison of the measured load-deflection curves for specimen DF\_N3 and two identical footings without (DF13<sup>6-8</sup>) and with stirrups as punching shear reinforcement (DF18<sup>6-8</sup>) is shown. The concrete compressive strength of the compared specimens was nearly the same and varied between  $f_{c,cyl} = 20.5$  MPa (2973 psi) and 21.7 MPa (3147 psi). The area of punching shear reinforcement up to  $0.8d$  was  $A_{v,0.8d} = 9040$  mm<sup>2</sup> (14.0 in.<sup>2</sup>) for specimen DF18. While specimen DF18 was designed to reach the maximum punching shear resistance, specimen DF\_N3 was designed to fail in punching shear inside the shear-reinforced zone.

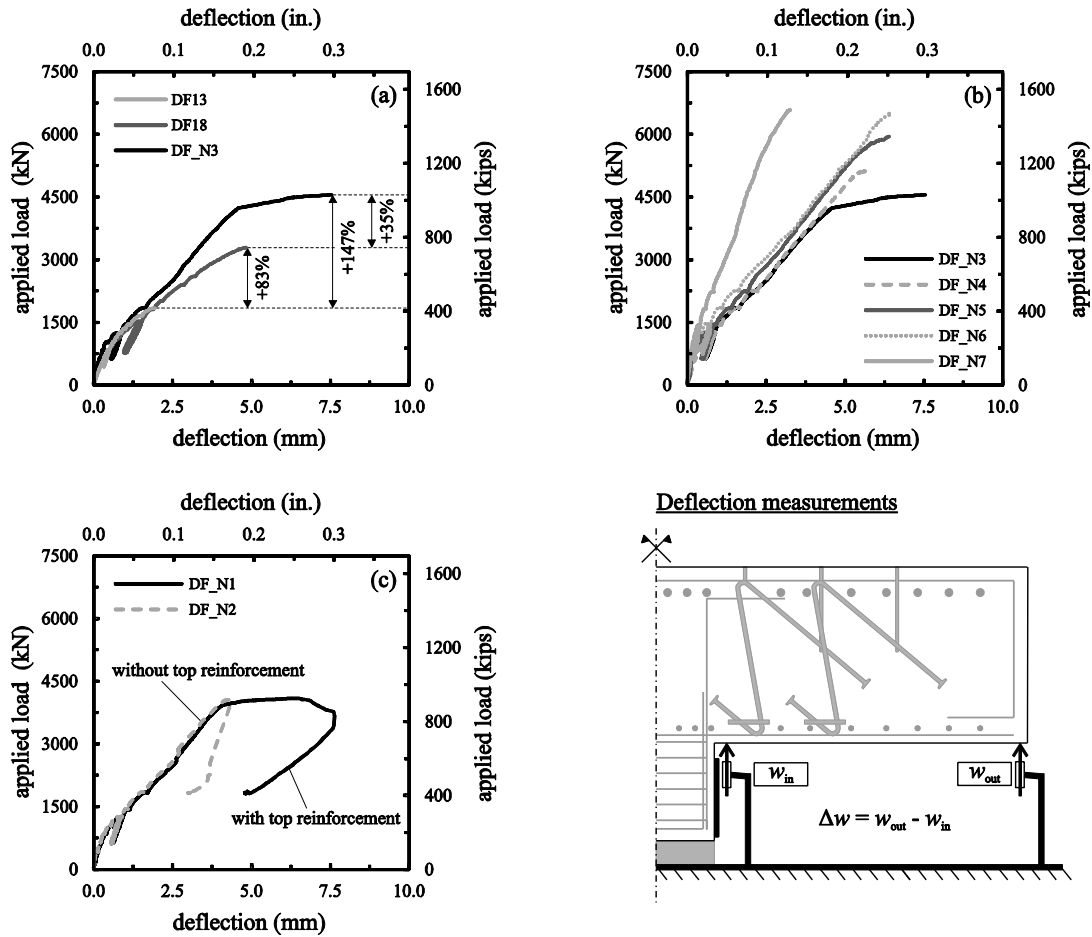


Fig. 4 Measured load-deflections curves

After a stiff initial response, first bending cracks appeared, leading to a reduced stiffness for the compared footings. Specimen DF13 failed in punching shear at 1839 kN (413 kips) and specimen DF18 failed in punching shear at 3361 kN (756 kips). The load-increase with stirrups as punching shear reinforcement (DF18) is 83% compared to specimen DF13 without punching shear reinforcement. Specimen DF\_N3 with the new punching shear reinforcement system shows a similar load-deflection curve up to approximately 1500 kN (337 kips). At higher load level, the gradient of the load-deflection curve is steeper compared to specimens DF13 and DF18 and the load-deflection curve finally becomes nearly horizontal, reflecting the observed ductile failure in punching shear at 4544 kN (1022 kips). As punching shear failure inside the shear-reinforced zone occurred, the load-increase with the new punching shear reinforcement system was 147% compared to specimen DF13 without punching shear reinforcement and 35% compared to specimen DF18, including stirrups as punching shear reinforcement.

The measured load-deflections curves of the footings with the new punching shear reinforcement consisting of 10 mm (0.4 in.) bars are shown in Fig. 4 (b). Regardless of the specific column perimeter  $u_0/d$  and the layout of the punching shear reinforcement, a stiff initial response corresponding to the uncracked stage could be observed. At approximately 800 kN (180 kips), first bending cracks appeared, leading to a reduced stiffness but still to a

nearly linear trend of the load-deflection curves. The gradient of the load-deflection curves of the specimens with a shear span-depth ratio  $a_v/d = 2.00$  is comparable. In contrast, as observed in previous test series<sup>6-8</sup> the gradient of specimen DF\_N7 with a shear span-depth ratio  $a_v/d = 1.25$  is much steeper.

In Fig. 4 (c), the load-deflection curves for the specimens with the new punching reinforcement consisting of 12 mm (0.5 in.) bars are shown. The comparison of the load-deflection curves for the identical specimens DF\_N1 (with top reinforcement) and DF\_N2 (without top reinforcement) shows a similar behavior until final failure took place. While specimen DF\_N1 failed at 4082 kN (918 kips) after further increase of the vertical deflection, specimen DF\_N2 failed at 4054 kN (911 kips) in a more brittle manner. However, both specimens nearly reached the same ultimate load (Table 1), confirming the assumption that a longitudinal reinforcement at the compression side does not significantly affects the punching shear capacity<sup>19</sup>.

INCREASE OF SLAB THICKNESS

The increase of the slab thickness is shown for three specimens in Fig. 5.

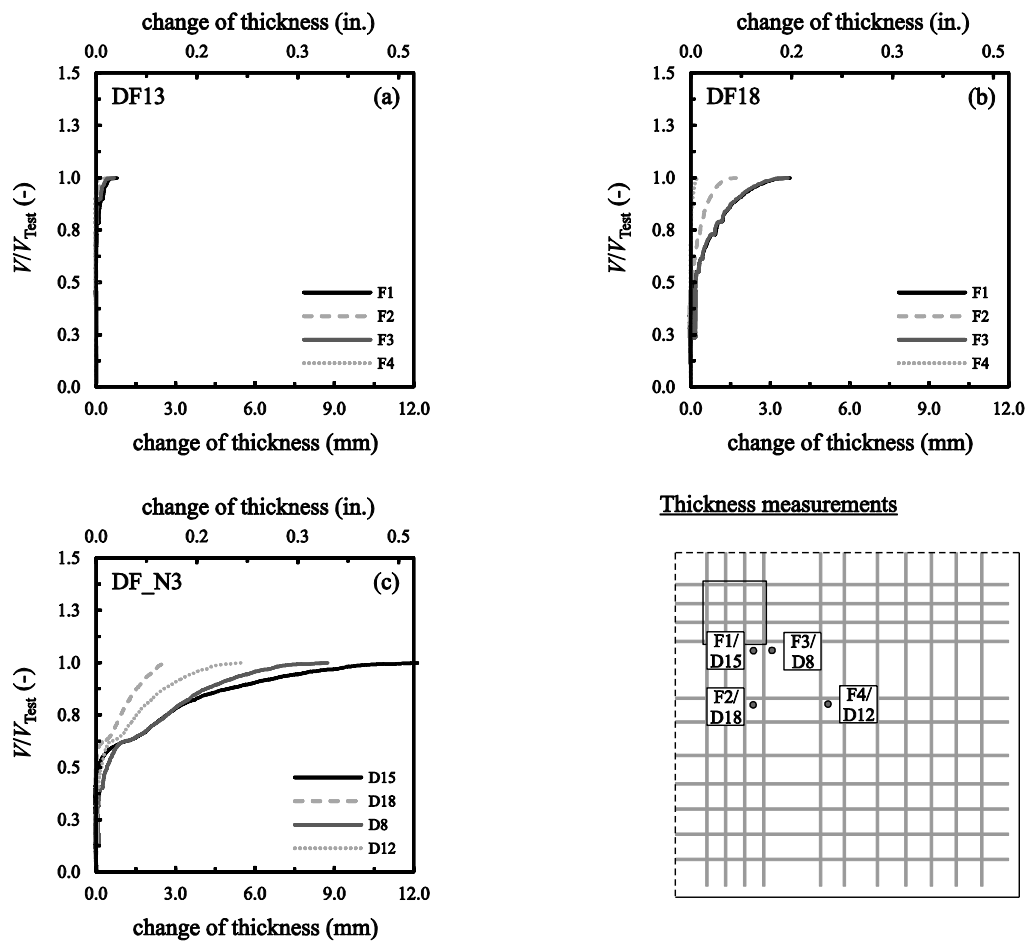


Fig. 5 Measured increase of slab thickness for test specimens DF13<sup>6-8</sup> (a), DF18<sup>6-8</sup> (b), and DF\_N3 (c)

The inner shear crack formation is indicated by a pronounced decrease of the inclination of the curves. In test specimen DF13 without punching shear reinforcement, the shear crack initiated at approximately 75% of the ultimate failure load  $V_{Test}$  and reached a maximum value of 0.8 mm (0.031 in.). In contrast, in the specimens with punching shear reinforcement, the shear crack initiated at approximately 35% of the ultimate failure load  $V_{Test}$ . This indicates that the shear reinforcement was able to control the crack width of the shear cracks. The maximum measured increase of the slab thickness was approximately 3.7 mm (0.145 in.) for specimen DF18 and 12.2 mm (0.480 in.) for specimen DF\_N3.

STRAINS OF PUNCHING SHEAR REINFORCEMENT

Fig. 6 shows exemplarily the measured tensile strains of the punching shear reinforcement elements in the first row for test specimens DF\_N4 (Layout I), DF\_N5 (Layout II), and DF\_N7 (Layout I\*). Specimen DF\_N7 was tested with a shear span-depth ratio of  $a_v/d = 1.25$ . Hence, a second row of punching shear reinforcement could not be installed due to lack of space. The strains corresponding to the yield strength of the punching shear reinforcement are indicated in the diagrams.

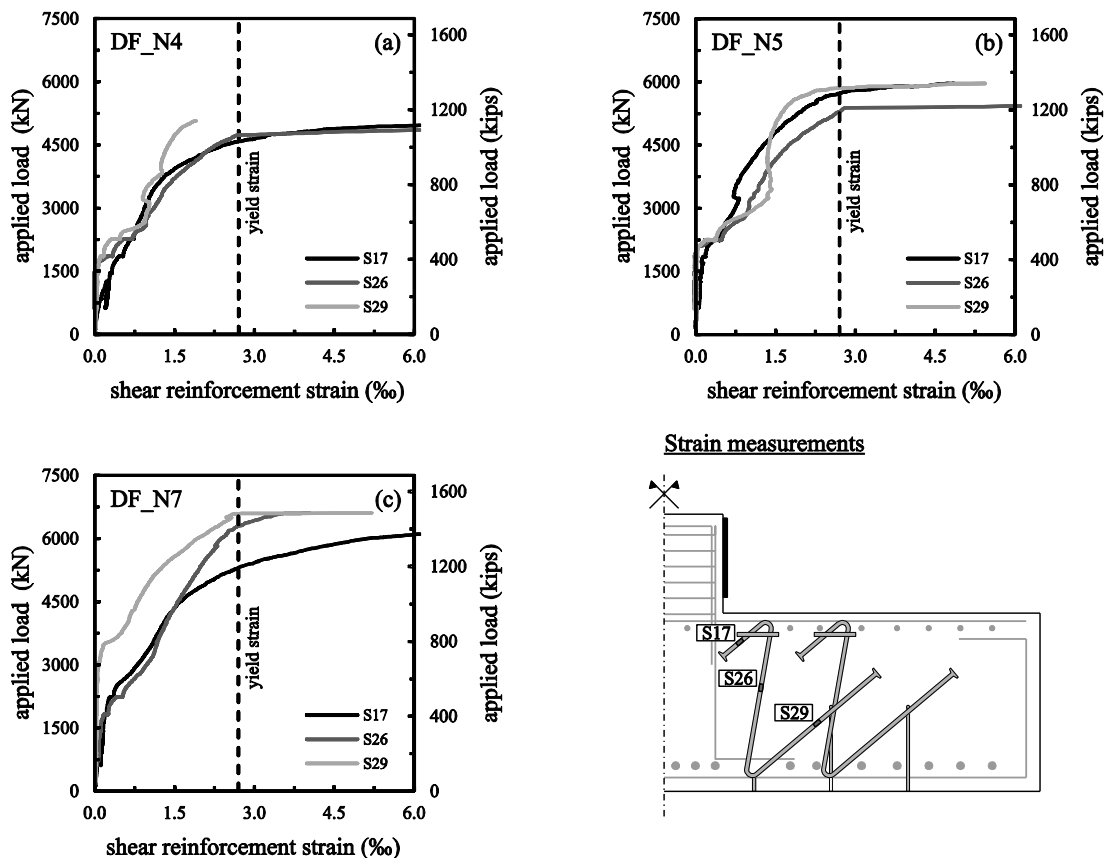


Fig. 6 Measured strains of punching shear reinforcement in the first row for test specimens DF\_N4 (a), DF\_N5 (b), and DF\_N7 (c)

In the tests, substantial steel strains were first observed at a load level coinciding more or less with the beginning of the inner shear crack formation. This was confirmed by the measured increase of the slab thickness at some load level. Regardless of the layout of the punching shear reinforcement, the measuring points in close vicinity of the column face (S17, S26) reached the yield strength before final failure took place. While for specimen DF\_N4 the value for the furthestmost measuring point from the column face (S29) was below the yield strength of the steel, specimens DF\_N5 and DF\_N7 reached the yield strength before the footing failed in punching shear.

Fig. 7 depicts the measured steel strains of the second row of punching shear reinforcement for test specimens DF\_N4 (Layout I), DF\_N5 (Layout II), and DF\_N6 (Layout I). In the tests with eight punching shear reinforcement elements in the second row, the recorded values were clearly below the yield strain of the steel. Specimen DF\_N5 with four punching shear reinforcement elements in the second row reached the yield strength when the footing failed in punching shear. The crack pattern of specimen DF\_N5 (Fig. 4 (4)) showed more cracks with large crack widths, especially outside the first row of punching shear reinforcement, which confirms this observation. However, regardless of the layout of the punching shear reinforcement, the measured steel strains (for all specimens larger than 1.0‰) confirm that the second row contributed to the punching shear resistance.

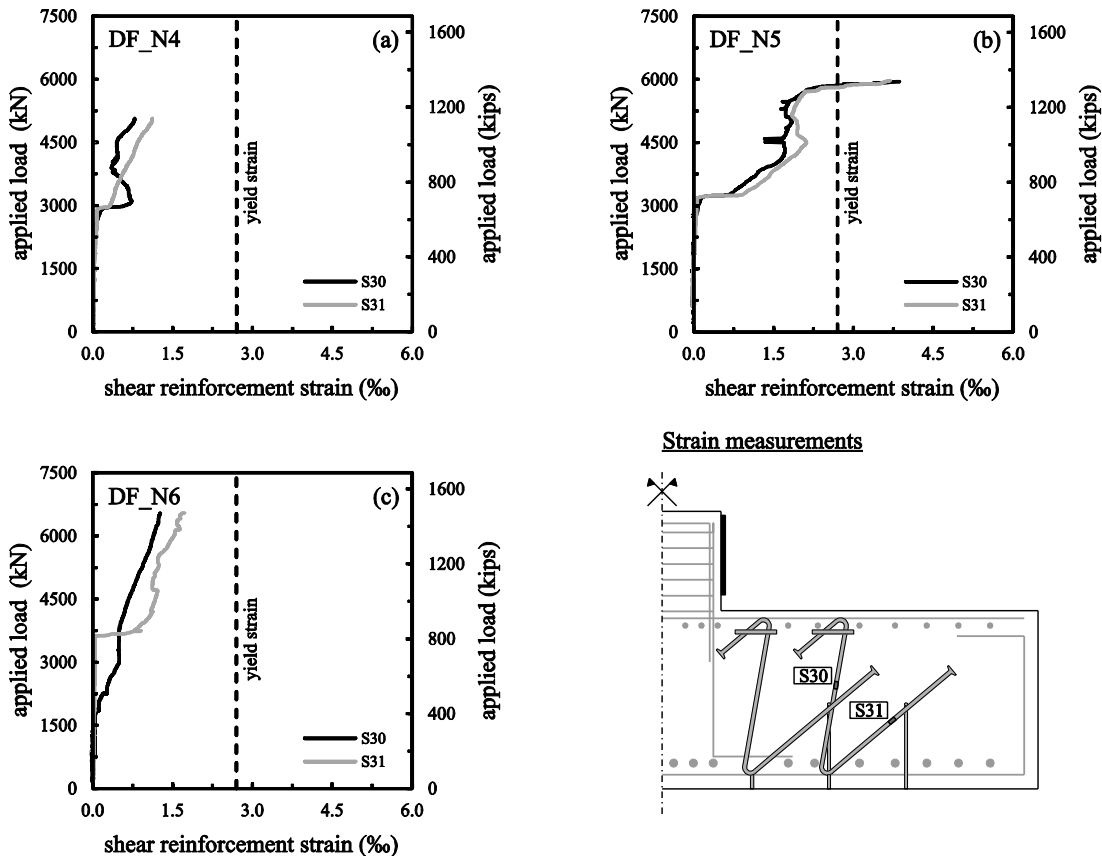


Fig. 7 Measured strains of punching shear reinforcement in the second row for test specimens DF\_N4 (a), DF\_N5 (b), and DF\_N6 (c)

The evaluation of the tensile strains of the punching shear reinforcement in both rows (Fig. 6, Fig. 7) and the crack patterns (Fig. 3) indicates a punching shear failure inside the shear-reinforced zone, regardless of the chosen layout of the punching shear reinforcement or its diameter. Thus, higher punching shear capacities at maximum load level might be obtained by installation of punching shear reinforcement elements with bigger diameters.

## COMPARISON OF PREDICTIONS AND EXPERIMENTAL RESULTS

ACI 318-14<sup>20</sup> do not differentiate between the punching shear design of flat slabs and footings. While for slabs without shear reinforcement the punching shear capacity mainly depends on the concrete strength, for slabs with shear reinforcement the punching shear capacity inside and outside the shear-reinforced zone as well as the maximum punching shear capacity has to be verified. The punching shear capacity of shear-reinforced slabs is highly influenced by the anchorage performance of the punching shear elements used. In this context, the punching shear provisions according to ACI 318-14<sup>20</sup> differentiate between the design of slabs with stirrups and studs.

### PUNCHING SHEAR PROVISIONS ACCORDING TO ACI 318-14

The control section is at  $d/2$  from the column face. The design is based on

$$v_u < \phi v_n \quad (1)$$

where  $\phi$  is a strength reduction factor (0.75 for shear);  $v_u$  is the applied factored shear stress using load factors according to ACI 318-14, Chapter 5.3 (Load factors and combinations); and  $v_n$  is the nominal shear resistance. The applied shear stress due to factored concentric shear force  $V_u$  is calculated as

$$v_u = V_u / (b_0 d) \quad (2)$$

where  $b_0$  is the perimeter of the critical section, and  $d$  is the distance from the extreme compression fiber to the centroid of tension reinforcement (effective depth). The shear resistance of the concrete  $v_c$  is the smallest value obtained from Eq. (3), (4), and (5)

$$v_c = 0.17(1 + 2/\beta_c)\lambda\sqrt{f'_c} \text{ MPa} = (2 + 4/\beta_c)\lambda\sqrt{f'_c} \text{ psi} \quad (3)$$

$$v_c = 0.083(\alpha_s d/b_0 + 2)\lambda\sqrt{f'_c} \text{ MPa} = (\alpha_s d/b_0 + 2)\lambda\sqrt{f'_c} \text{ psi} \quad (4)$$

$$v_c = 0.33\lambda\sqrt{f'_c} \text{ MPa} = 4\lambda\sqrt{f'_c} \text{ psi} \quad (5)$$

where  $\alpha_s$  is a parameter taken as 40 for interior, 30 for edge, and 20 for corner columns;  $\beta_c$  is the ratio of long to short side of concentrated load or reaction area;  $\lambda$  is a factor accounting for the concrete density; and  $b_0$  is the perimeter of the control section. For slabs without shear

reinforcement, the nominal shear resistance  $v_n$  in Eq. (1) equals  $v_c$ . The isolated footing may be assumed to be rigid, resulting in a uniform soil pressure for concentric loading. The shear force can be reduced by the effective soil pressure within the control perimeter.

If  $v_u > \phi v_n$ , shear reinforcement has to be used. Two control sections are to be checked:  $d/2$  from the column face and  $d/2$  from the outermost row of shear reinforcement. The punching shear resistance inside the shear-reinforced zone is calculated as

$$v_n = v_c + v_s \leq v_{\max} \quad (6)$$

where  $v_{cs}$  is the shear stress resisted by the concrete inside the shear-reinforced zone,  $v_s$  is the shear stress resisted by the shear reinforcement, and  $v_{\max}$  is the maximum allowed shear stress.

Acknowledging the superior anchorage performance of shear studs, ACI 318-14 distinguishes between shear studs and stirrups as shear reinforcement. The nominal shear strength provided by concrete  $v_{cs}$  inside the shear-reinforced zone is calculated as

$$v_c = 0.17\lambda\sqrt{f'_c} \text{ MPa} = 2\lambda\sqrt{f'_c} \text{ psi (for stirrups)} \quad (7)$$

$$v_c = 0.25\lambda\sqrt{f'_c} \text{ MPa} = 3\lambda\sqrt{f'_c} \text{ psi (for studs)} \quad (8)$$

The nominal shear strength provided by vertical shear reinforcement elements  $v_s$  is calculated as

$$v_s = (A_v f_{yt}) / (b_0 s) \quad (9)$$

where  $A_v$  is the area of shear reinforcement in one row around the column,  $s$  is the spacing of the shear reinforcement, and  $f_{yt}$  is the yield strength of the shear reinforcement not to exceed 413 MPa (60,000 psi). Where inclined shear reinforcement elements are used, the nominal shear strength  $v_s$  can be calculated in accordance with the equation for one-way shear as

$$v_s = (A_v f_{yt} (\sin\alpha + \cos\alpha)) / (b_0 s) \quad (10)$$

where  $\alpha$  is the angle between inclined shear reinforcement elements and longitudinal axis of the member. For studs as punching shear reinforcement, a minimum amount of shear reinforcement according to the following equation shall be provided

$$A_v / s \geq 0.17\sqrt{f'_c} b_0 / f_{yt} \text{ MPa} = 2\sqrt{f'_c} b_0 / f_{yt} \text{ psi} \quad (11)$$

The maximum allowed shear stress  $v_{\max}$  is determined as

$$v_{\max} = 0.50\lambda\sqrt{f'_c} \text{ MPa} = 6\lambda\sqrt{f'_c} \text{ psi (for stirrups and studs with } s \leq 0,75d) \quad (12)$$

$$v_{\max} = 0.67\lambda\sqrt{f'_c} \text{ MPa} = 8\lambda\sqrt{f'_c} \text{ psi (for studs with } s \leq 0,5d) \quad (13)$$

Outside the shear-reinforced zone, the shear stress resistance of concrete is limited to the one-way shear strength value of

$$v_c = 0.17\lambda\sqrt{f'_c} \text{ MPa} = 2\lambda\sqrt{f'_c} \text{ psi} \quad (14)$$

## COMPARISON WITH ACI 318-14

For the comparison between the present tests and the punching shear provisions according to ACI 318-14<sup>20</sup>, all material and strength reduction factors in the code equations are taken as unity. For a comparison with tests results, the control of the crack width is not relevant, thus the yield strength applied to the shear reinforcement is not limited to 413 MPa (60,000 psi). The ultimate recorded test loads considering the effective soil pressure within the control perimeter are compared with the values predicted by ACI 318-14<sup>20</sup> in Table 2.

Table 2 Comparison of predictions<sup>20</sup> and experimental results

Test	$b_0$	$v_{c, \text{studs}}$	$A_{v, 1.0d}$	$v_s$	$v_{n, \text{studs}}$	$v_{\text{max, studs}}$	$v_{\text{ACI, studs}}$	governing?	$V_{\text{Test, red}}$	$V_{\text{ACI, studs}}$	$V_{\text{Test, red}} / V_{\text{ACI, studs}}$
	<b>m</b>	<b>MPa</b>	<b>mm<sup>2</sup></b>	<b>MPa</b>	<b>MPa</b>	<b>MPa</b>	<b>MPa</b>	-	<b>kN</b>	<b>kN</b>	-
	<b>(in.)</b>	<b>(psi)</b>	<b>(in<sup>2</sup>)</b>	<b>(psi)</b>	<b>(psi)</b>	<b>(psi)</b>	<b>(psi)</b>	-	<b>(kips)</b>	<b>(kips)</b>	-
DF_N1	2.40 (94.5)	1.186 (172.0)	9291 (14.4)	2.265 (328.5)	3.451 (500.5)	3.178 (460.9)	3.178 (460.9)	$v_{\text{max}}$	3628 (816)	3051 (686)	1,19
DF_N2	2.40 (94.5)	1.188 (172.3)	9291 (14.4)	2.265 (328.5)	3.453 (500.8)	3.185 (462.0)	3.185 (462.0)	$v_{\text{max}}$	3604 (810)	3058 (688)	1,18
DF_N3	2.40 (94.5)	1.132 (164.2)	6452 (10.0)	1.471 (213.4)	2.603 (377.5)	3.034 (440.0)	2.603 (377.5)	$v_c + v_s$	4039 (908)	2498 (562)	1,62
DF_N4	2.80 (110.2)	1.129 (163.7)	6452 (10.0)	1.261 (182.9)	2.390 (346.6)	3.026 (438.9)	2.390 (346.6)	$v_c + v_s$	4360 (980)	2676 (602)	1,63
DF_N5	2.80 (110.2)	1.255 (182.0)	5724 (8.9)	1.129 (163.7)	2.384 (345.8)	3.363 (487.8)	2.384 (345.8)	$v_c + v_s$	5131 (1154)	2670 (600)	1,92
DF_N6	3.20 (126.0)	1.151 (166.9)	6452 (10.0)	1.113 (161.4)	2.264 (328.4)	3.085 (447.4)	2.264 (328.4)	$v_c + v_s$	5473 (1230)	2898 (652)	1,89
DF_N7	2.80 (110.2)	1.194 (173.2)	4997 (7.7)	0.985 (142.9)	2.179 (316.0)	3.199 (464.0)	2.179 (316.0)	$v_c + v_s$	4667 (1049)	2440 (549)	1,91

$b_0$ : control perimeter according to ACI 318-14<sup>20</sup>;  $v_{c, \text{studs}}$ : nominal shear strength provided by concrete inside the shear-reinforced zone according to Eq. (8);  $v_s$ : nominal shear strength provided by inclined shear reinforcement elements according to Eq. (10);  $v_{\text{max, studs}}$ : maximum allowed shear stress according to Eq. (12);  $v_{\text{ACI, studs}}$ : minimum value of  $v_{n, \text{studs}}$  and  $v_{\text{max, studs}}$ ;  $V_{\text{Test, red}}$ : ultimate failure load reduced by the effective soil pressure within the control perimeter ( $V_{\text{Test, red}} = V_{\text{Test}}(1 - A_{\text{cont}}/A)$ );  $V_{\text{Test, red}} / V_{\text{ACI, studs}}$ : ratio of experimental and predicted failure load according to ACI 318-14<sup>20</sup>.

Due to the good anchorage performance of the new punching shear reinforcement elements (Fig. 6), the nominal shear strength provided by concrete inside the shear-reinforced zone  $v_{cs}$  and the maximum allowed shear stress  $v_{\text{max}}$  are calculated following the code provisions for studs (Eq. (8) and (13)). The nominal shear strength provided by the inclined punching shear reinforcement elements  $v_s$  is calculated in accordance with Eq. (10). Except for the short

inclined bars in the second row, all bars of the punching shear reinforcement elements within a distance  $1.0d$  from the column face were considered for the calculation of  $v_s$ .

The calculation of the punching shear capacity according to ACI 318-14<sup>20</sup> leads for all tests to a safe estimation of the ultimate recorded failure load. While the specimens with 10 mm (0.4 in.) bars failed inside the shear-reinforced zone, for specimen DF\_N1 and DF\_N2 with 12 mm (0.5 in.) bars the maximum allowed shear stress  $v_{\max}$  according to ACI 318-14<sup>20</sup> is governing. However, especially for a failure inside the shear-reinforced zone, the code provisions are conservative. This could be attributed to the decreased shear strength provided by concrete for shear-reinforced slabs ( $v_{cs, studs} = 0.75v_c$ ). The good anchorage performance and the s-shaped form of the new punching shear reinforcement elements allow the shear crack widths do be efficiently controlled. Hence, a higher concrete contribution compared to vertical punching shear reinforcement elements, maybe in combination with a strut-and-tie model with flatter inclined compressive struts, might be achieved. To verify this assumption, further experimental investigations especially at maximum load level are necessary.

## CONCLUSIONS

The results of the experimental investigations on reinforced concrete footings with a new punching shear reinforcement system allow the following conclusions to be drawn:

1. The new punching shear reinforcement system with inclined bars significantly increases the punching shear capacity of reinforced concrete footings. The high load-increase of 147% compared to identical footings without punching shear reinforcement is approximately 40% higher than for stirrups.
2. The presented specimens failed in punching shear inside the shear-reinforced zone. Higher punching shear capacities at maximum load level might be obtained by installation of punching shear reinforcement elements with bigger diameters.
3. Regardless of the layout of the punching shear reinforcement, the measured steel strains confirm that the second row contributed to the punching shear resistance.
4. By installation of longitudinal reinforcement at the compression side, a more ductile failure in punching shear can be observed.
5. The punching shear provisions according to ACI 318-14 lead to a safe estimation of the punching shear capacity of footings with the new punching shear reinforcement system.
6. Due to the good anchorage performance and the s-shaped form of the new punching shear reinforcement elements, a higher concrete contribution compared to the provisions of ACI 318-14 for shear-reinforced slabs might be achieved.

## ACKNOWLEDGMENTS

The investigations presented were supported by the German Research Foundation (Deutsche Forschungsgemeinschaft, DFG-GZ HE 2637/18-1) and the authors wish to express their sincere gratitude.

**REFERENCES**

1. Talbot, A.N., "Reinforced Concrete Wall Footings and Column Footings," *Publications of the Engineering Experiment Station*, Bulletin No. 67, 1913.
2. Richart, F.E., "Reinforced Concrete Wall and Column Footings," *Journal of the American Concrete Institute*, V. 20, No. 2, 1948, pp. 97-127 (Part 1), No. 3, 1948, pp. 237-261 (Part 2).
3. Dieterle, H., Steinle, A., "Blockfundamente für Stahlbetonfertigstützen," *Deutscher Ausschuss für Stahlbeton*, Heft 326, 1981.
4. Dieterle, H., Rostásy, F.S., "Tragverhalten quadratischer Einzelfundamente aus Stahlbeton," *Deutscher Ausschuss für Stahlbeton*, Heft 387, 1987.
5. Hallgren, M., Kinnunen, S., Nylander, B., "Punching Shear Tests on Column Footings," *Nordic Concrete Research*, V. 21, No. 3, 1998, pp. 1-22.
6. Hegger, J., Sherif, A.G., Ricker, M., "Experimental Investigations on Punching Behavior of Reinforced Concrete Footings," *ACI Structural Journal*, V. 103, No. 4, July-August 2006, pp. 604-613.
7. Hegger, J., Ricker, M., Sherif, A.G., "Punching Strength of Reinforced Concrete Footings," *ACI Structural Journal*, V. 106, No. 5, September-October 2009, pp. 706-716.
8. Siburg, C.; Hegger, J., "Experimental investigations on the punching behaviour of reinforced concrete footings with structural dimensions," *Structural Concrete*, V. 15, No.3, 2014, pp. 331-339.
9. Beutel, R., Hegger, J., "The effect of anchorage on the effectiveness of the shear reinforcement in the punching zone," *Cement and Concrete Composites*, V. 24, No. 6, December 2002, pp. 539-549.
10. Ruiz, M.F., Muttoni, A., "Applications of Critical Shear Crack Theory to Punching of Reinforced Concrete Slabs with Transverse Reinforcement," *ACI Structural Journal*, V. 106, No. 4, July-August 2009, pp. 485-494.
11. Hegger, J., Häusler, F., Ricker, M., "Zur maximalen Durchstantragfähigkeit von Flachdecken," *Beton- und Stahlbetonbau*, V. 102, No. 11, November 2007, pp. 770-777.
12. Andrä, H.P., "Zum Tragverhalten von Flachdecken mit Dübelleisten-Bewehrung im Auflagerbereich," *Beton- und Stahlbetonbau*, V. 76, No. 3, March 1981, pp. 53-57 (Part 1), No. 4, April 1981, pp.100-104 (Part 2).
13. Mokhtar, A.S., Ghali, A., Dilger, W., "Stud shear reinforcement for flat concrete plates," *ACI Journal, Proceedings*, V. 82, No. 5, September 1985, pp. 676-683.
14. Ricker, M., Häusler, F., "European punching design provisions for double-headed studs," *Structures and Buildings*, V. 167, No. SB8, August 2014, pp. 495-506.
15. Ferreira, M.P., Melo, G.S., Regan, P.E., Vollum, R.L., "Punching of Reinforced Concrete Flat Slabs with Double-Headed Shear Reinforcement," *ACI Structural Journal*, V. 111, No. 2, March-April 2014, pp.363-374.

16. DIN EN 1992-1-1:2011-01, “Eurocode 2: Bemessung und Konstruktion von Stahlbeton- und Spannbetontragwerken – Teil 1-1: Allgemeine Bemessungsregeln und Regeln für den Hochbau,” Deutsche Fassung EN 1992-1-1:2004 + AC:2010, 2011.
17. DIN EN 1992-1-1/NA:2013-04, “Nationaler Anhang – National festgelegte Parameter – Eurocode 2: Bemessung und Konstruktion von Stahlbeton- und Spannbetontragwerken – Teil 1-1: Allgemeine Bemessungsregeln und Regeln für den Hochbau,” Deutsche Fassung EN 1992-1-1/NA: 2013-04, 2013.
18. Gesund, H., “Flexural Limit Analysis of Concentrically Loaded Column Footings,” *ACI Journal, Proceedings*, V. 80, No. 3, May-June 1983, pp. 223-228.
19. Beutel, R., “Durchstanzen schubbewehrter Flachdecken im Bereich von Innenstützen,” PhD thesis, RWTH Aachen University, Institute of Structural Concrete, 2003. (in German)
20. ACI Committee 318, “Building Code Requirements for Structural Concrete (ACI 318-14) and Commentary (ACI 318R-14),” American Concrete Institute, Farmington Hills, MI, 2014.